Published in final edited form as:
*Mol Imaging*. 2007 ; 6(6): 384–392.

# Tailoring the Size Distribution of Ultrasound Contrast Agents: Possible Method for Improving Sensitivity in Molecular Imaging

**Esra Talu**, **Kanaka Hettiarachchi**, **Shukui Zhao**, **Robert L. Powell**, **Abraham P. Lee**, **Marjorie L. Longo**, and **Paul A. Dayton**
From the Departments of Chemical Engineering and Materials Science and Biomedical Engineering, University of California, Davis, Davis, CA; and Department of Biomedical Engineering, University of California, Irvine, Irvine, CA

## Abstract

Encapsulated microbubble contrast agents incorporating an adhesion ligand in the microbubble shell are used for molecular imaging with ultrasound. Currently available microbubble agents are produced with techniques that result in a large size variance. Detection of these contrast agents depends on properties related to the microbubble diameter such as resonant frequency, and current ultrasound imaging systems have bandwidth limits that reduce their sensitivity to a polydisperse contrast agent population. For ultrasonic molecular imaging, in which only a limited number of targeted contrast agents may be retained at the site of pathology, it is important to optimize the sensitivity of the imaging system to the entire population of contrast agent. This article presents contrast agents with a narrow size distribution that are targeted for molecular imaging applications. The production of a functionalized, lipid-encapsulated, microbubble contrast agent with a monodisperse population is demonstrated, and we evaluate parameters that influence the size distribution and demonstrate initial acoustic testing.

*Molecular imaging with ultrasound* uses targeted ultrasound contrast agents. These contrast agents are injected intravascularly and are retained on the endothelium at the site of pathology via adhesion ligands incorporated into the agent shell. Although some targeted ultrasound contrast agents consist of liquid-based particles,[1–3] the majority of targeted contrast agents are encapsulated microbubbles owing to their substantially higher echogenicity than liquid-based agents.[4–8] These agents incorporate targeting ligands into their exterior shell, such as antibodies, peptides, peptidomimetics, or glycoconjugates, which are chosen for specificity to molecular markers of disease.[9,10] After intravascular injection, targeted contrast agents bind to endothelial cells at the site of pathology. Target pathologies for ultrasonic molecular imaging must involve ligands expressed intravascularly owing to the diameter of these large (1–10 microns) contrast agents, and proposed targets include angiogenesis, thrombus, and inflammation.[4,5,11–13]

Molecular imaging with ultrasound is a relatively new concept; only within the past few years has research progressed to the point of studies in animal models. Initial investigations into the use of targeted ultrasound contrast agents have clearly demonstrated proof of concept; however, researchers using intravital microscopy and histology have observed that only a small percentage of the initial dose of targeted microbubbles are retained in the tissue.[4,7,12,14] Although researchers are currently working on other methods to improve this sensitivity, such as increasing contrast retention using improved adhesion mechanisms,[5,7,15]

Address reprint requests to: Paul Dayton, PhD, Joint Department of Biomedical Engineering, UNC-Chapel Hill, MacNider Bldg, CB #7575, Chapel Hill, NC 27599-7575; e-mail: padayton@email.unc.edu.

delivering a higher payload of contrast agents to the target site,[16,17] and improving signal processing and detection algorithms,[18,19] little has been done toward optimization of the contrast agents themselves.

Common methods to generate lipid-encapsulated microbubble contrast agents, such as sonication and mechanical agitation, result in production of polydisperse microbubbles. Definity, an agent approved by the US Food and Drug Administration (FDA), is described in the package insert as having a mean diameter of 1.1 to 3.3 mm with a maximum microbubble diameter of 20 μm.[20]

Microbubble contrast agents work on the principle that owing to their compressible gas core, they scatter incident acoustic waves more efficiently than surrounding blood and tissue. Given that the resonant frequency of a microbubble is directly related to its size, and available ultrasound systems have limited frequency bandwidth, a clinical imaging system is optimized only for a small percentage of a polydisperse contrast agent population. For blood pool (nontargeted) contrast imaging, this is not a problem owing to the large number of microbubbles injected into circulation ($10^8$–$10^{10}$), where many of the microbubbles are within the diameter range optimized for detection. However, for targeted imaging, in which only a small number of agents are retained at the site of pathology, it is important to have all of the contrast agents optimized for detection by the imaging system.

Previous studies have demonstrated that a microfluidic technique called flow focusing can be used to generate size-controlled monodisperse microbubbles.[21,22] Flow focusing operates on the principle that a stream of gas is focused by the flow of a liquid through an orifice, where the thread breaks and releases a continuous stream of microbubbles. Microbubble size can be precisely controlled by adjusting the gas and liquid flow rates. Here we use this microfluidic technique to produce a new type of lipid-stabilized monodisperse contrast agent that is functionalized for molecular imaging. We demonstrate the advantages of this agent through simulations, proof-of-concept targeting to $\alpha_v\beta_3$-expressing cells, and first acoustic results from interrogation of a monodisperse agent compared with a polydisperse agent.

## Materials and Methods

### Simulations

The resonant frequency of a microbubble is directly related to its diameter. A microbubble that is driven at its resonant frequency responds to ultrasonic excitation much more efficiently than one that is driven off-resonance. For a group of microbubbles, the percentage of the population with resonant frequencies that fall within the bandwidth of a transducer indicates the efficiency of the imaging system to detect the signals from this microbubble population. To measure this efficiency, different transducer bandwidths were simulated, with frequency ranges from 1 to 10 MHz, each with fractional bandwidths of 80%. Also, a 3.8 MHz transducer was simulated as a best-case example since 3.8 MHz is approximately the resonant frequency of a 2.1 μm microbubble—approximately the median size experimentally measured from a sample of the commercially available lipid-shelled contrast agent Definity (Bristol Myers Squibb, N. Billerica MA).

The distribution of linear resonant frequencies for populations of polydisperse and monodisperse microbubbles was simulated using *Matlab* (The Mathworks Inc, Natick, MA). Resonant frequencies for lipid-encapsulated microbubbles were calculated using the formulation described by Morgan and colleagues.[23] Size distributions were assumed to be Gaussian, which is a reasonable assumption based on our experimental observations. The size distribution for the polydisperse microbubbles was matched to the size distribution of Definity measured experimentally. The mean diameter of the monodisperse microbubbles

was varied according to the transducer center frequency, and a standard deviation was set to 5% of the mean size, as determined experimentally.

### Flow-Focusing Chamber

Flow-focusing chambers made out of polydimethylsiloxane (PDMS) were used to produce microbubbles less than 10 μm in diameter. Microfabrication of PDMS chambers with an orifice diameter of 10 μm and gas and liquid channel widths of 35 and 50 μm, respectively, was previously described by Hettiarachchi and colleagues.[24] The channels were filled with deionized (DI) water immediately after sealing to ensure the hydrophilic character of the walls of microchannels. Liquid flow rates were provided by a high-precision Harvard Apparatus (Holliston, MA) syringe pump calibrated to within ± 0.35%. Nitrogen gas was introduced from a compressed gas cylinder via a low-pressure regulator accurate within 0.2 psi. By adjusting the liquid and gas flow rates, the mean diameter of the microbubbles produced can be precisely controlled.[24,25]

### Microbubble Formulation

Stabilized microbubbles were formulated using lipid components similar to those previously described for the research production of ultrasound contrast agents.[26–29] Briefly, 1,2-distearoyl-*sn*--glycero-3-phosphocholine (DSPC) and 1,2-distearoyl-*sn*-glycero-3-phosphoethanola-mine-N-[methoxy(polyethylene glycol)-2000] (DSPE-PEG2000) were purchased from Avanti Polar Lipids (Alabaster, AL). Viscosity control was achieved using glycerin and propylene glycol (GP) purchased from Sigma-Aldrich (St. Louis, MO). The lipid composition contained 0.5 mg/mL DSPC with a 9:1 mol:mol ratio of DSPC to DSPE-PEG2000. The fluorescent probe, $^{3}$H-indolium, 2-[3-(1,3-dihydro-3,3-dimethyl-1-octadecyl-2H-indol-2-yli-dene)-1-propenyl]-3,3-dimethyl-1-octadecyl-, perchorate (DiI), was purchased from Molecular Probes (Eugene, OR). DiI was added to the DSPC–DSPE-PEG2000 solution at a concentration of 0.4 μL/mL before the production of microbubbles.

### Functionalization of Microbubbles

DSPE-PEG2000-biotin was purchased from Avanti Polar Lipids. The lipid solutions were composed of 0.5 mg/mL DSPC with a 90:5:5 mol:mol:mol ratio of DSPC to DSPE-PEG2000 to DSPE-PEG2000-biotin. Fluorescein-conjugated avidin was purchased from Pierce (Rockford, IL). Ten microliters of fluorescently labeled avidin solution (5 mg/mL) was added to 500 μL of biotinylated microbubbles. After waiting for 5 minutes, free avidin was washed from the microbubble solution by exchanging the solution with fresh DI water using a pipette. This procedure was repeated twice, and microbubbles were placed on a microscope slide with a coverslip for observation. Fluorescence images were captured with a Cascade camera (512b, Photometrics, Tucson, AZ) on a microscope (IV600L, Mikron Instruments, San Diego, CA) and processed with SimplePCI (C-Imaging, Cranberry Township, PA).

### Size Characterization and Stabilization

A high-speed camera system (APS-RX, Photron, Inc., San Diego, CA) coupled to an inverted microscope (IX71, Olympus, Japan) was used to observe the microbubbles exiting the flow-focusing chamber as well as microbubble dissolution. Microbubbles produced at a liquid flow rate of 30 μL/min and a gas pressure of 2.5 psi were collected at the outlet of the microfluidic chip to perform size measurements. A minimum of 400 microbubbles were analyzed for distribution data using the *Scion Image* (Scion Corporation, Frederick, MD) program. The production rate of the microbubbles was measured from high-speed camera images.

For comparison with contrast agents made by flow focusing, a vial of Definity was purchased from Bristol-Myers Squibb Medical Imaging (North Billerica, MA). Microbubbles were formed by the shaking method using a CAPMIX mixing machine (ESPE, Seefeld, Germany) for 45 seconds according to the manufacturer's instructions. A minimum of 1,800 microbubbles were analyzed for distribution data using the *Scion Image* program. Size data were presented in terms of mean ± standard deviation.

Fluorescence images were captured with a Cascade camera on an upright microscope (IV600L) and processed with SimplePCI.

## Molecular Targeting

Monodisperse microbubbles targeted with arginine-glycine-aspartic acid (RGD) were produced with our flow-focusing chambers using a proprietary lipid formulation provided by ImaRx Therapeutics (Tucson, AZ). This formulation incorporates lipids bearing a cyclic-RGD bioconjugate that has previously been shown to form microbubbles, which demonstrate specific targeting to $\alpha_v\beta_3$-expressing cells, such as A375m.[30] A375m cell lines were obtained from John Marshall at Cancer Research UK Clinical Centre, London, and cultured and maintained using standard protocols.[11] Cells were grown until confluent on 25 mm square glass coverslips in a humidified tissue culture incubator at 37°C in a 5% $CO_2$/air atmosphere. Targeted monodisperse microbubbles were introduced into phosphate-buffered saline (PBS) at a concentration of approximately $1 \times 10^6$/mL and allowed to float into contact with the cell monolayer. After incubation with microbubbles for approximately 5 minutes, the cell coverslips were twice rinsed by gently swirling in a fresh PBS solution and examined under a light microscope.

## Acoustic Study

Echoes from single microbubbles produced in our laboratory using microfluidics (nearly monodisperse) or by the traditional mechanical agitation method (polydisperse) were recorded using a pulser/receiver system (Ritec SP-801 and BR-640A, Ritec, Warwick, RI) in conjunction with a diplexer (RDX-2, Ritec). A transducer with a nominal center frequency of 2.25 MHz (Panametrics V305, Waltham, MA) was used that had a −6 dB bandwidth of 1.75 to 3.45 MHz, a focal length of 2 inches, and an aperture size of 0.75 inches.

Microbubbles were pumped through a 200 μm cellulose tube with a syringe pump (Harvard Apparatus) at a mean velocity of 20 mm/s. The concentration was reduced by dilution until single-microbubble echoes were observed. The tube was held vertically to reduce microbubble accumulation along the wall owing to flotation, and the transducer was placed at an angle of about 60° with respect to the tube to eliminate reflected echoes from the tube wall. Received echoes were amplified by 40 dB, bandpass filtered between 1 and 12 MHz, and digitized at 125 MHz on a computer through a *LabView* (National Instruments Corporation, Austin, TX) interface. A pulse repetition frequency of 100 Hz was used.

The echoes were analyzed offline with *Matlab*. The maximum, minimum, and root mean square (RMS) value of each echo were calculated directly from the echo in the time domain. The mean center frequency of each echo was calculated in the frequency domain, and the correlation coefficients between each echo were calculated and averaged. The mean and variation of these parameters were reported.

# Results

## Simulations

A microbubble population with a size distribution similar to commercially available lipid-encapsulated contrast agents (diameter distribution of 2.1 ± 1.1 μm) was found to have only 49% of microbubbles whose resonant frequencies lie within the −6 dB bandwidth of a transducer with an optimized center frequency of 3.8 MHz (Figure 1A). This result indicates the “best case” for the transducer bandwidth overlapping the resonant frequency distribution of the microbubble population. For a population of monodisperse microbubbles with the same mean diameter and a standard deviation of 5% of the mean diameter, 100% of microbubbles have their resonant frequency within the transducer bandwidth (Figure 1B).

For higher imaging frequencies such as 5, 7, and 10 MHz, the percentage of microbubbles with resonant frequencies within the bandwidth decreases to 36%, 23%, and 18%, respectively. By tailoring monodisperse contrast agent size distribution to match the desired frequency, 100% of the population will have resonant frequencies that fall within the transducer bandwidth (Table 1).

## Production of Monodisperse Microbubbles in Size Range for Imaging

We produced lipid-coated monodisperse microbubbles with a microfluidic chip system using flow focusing, described previously.[24,31] The polydispersity of contrast agents manufactured in our laboratory using this technique is much less than the commercially available contrast agent Definity (3.7 ± 0.2 μm vs 2.7 ± 2.0 μm; Figure 2). Using lower gas pressures (less than 5 psi) and liquid flow rates (less than 60 μL/min) results in highly monodisperse microbubbles within the size range of ultrasound contrast agents. With a flow-focusing system, the size of the microbubbles primarily depends on the orifice size, gas pressure, and liquid flow rate. For a fixed liquid flow rate of 30 μL/min, an increase in gas pressure resulted in an increase in the size of the microbubbles (Figure 3). By changing the gas pressure, the production of monodisperse microbubbles can be tailored to the size desired for an imaging application. In addition to the orifice size, gas pressure, and liquid flow rate, the size of the microbubbles is affected by the bulk viscosity of the solution. For the case of 1% and 5 vol% GP, the size of the microbubbles is only minimally affected by the solution viscosity. However, for the 10 vol% GP case, smaller microbubbles were produced for the same flow rate parameters.

The production rate ranges between 100 and 50,000 microbubbles per second depending on the gas pressure and liquid flow rate as well as the bulk viscosity. Production rate increases with the gas pressure and liquid flow rate and decreases with the bulk viscosity of the solution (Table 2).

## Stabilizing Microbubbles for Use as Contrast Agents

Microbubbles were prepared using lipid shell and gas components similar to those used in commercially made ultrasound contrast agents and those described by other researchers.[32,33] The choice of shell material greatly affects microbubble stability, and the DSPC–DSPE-PEG2000 mixture for the stabilizing lipids was used for optimal stability.[31] Microbubbles were filled with nitrogen, and the solution surrounding the microbubbles was saturated with air in all experiments. Some degree (10–20%) of dissolution was observed within minutes of production, after which the population of monodisperse microbubbles was observed to remain stable over several hours.

Images of DSPC–DSPE–PEG2000-coated and nitrogen-filled microbubbles under a microscope slide were recorded. The average size of the microbubbles remained 3.7 μm with a standard deviation of 0.2 μm over the 8-hour observation period (Figure 4).

Fluorescence microscopy images of DSPC–DSPE–PEG2000-coated and nitrogen-filled microbubbles, using a lipid dye, DiI, demonstrate the presence of the lipid shell on the surface of the contrast agents produced by flow focusing (Figure 5, A and B). Additionally, the coexistence of condensed lipid-rich dark domains and expanded PEG-rich bright domains was observed at higher magnification owing to the partitioning of the fluorescent probe into the expanded phase (see Figure 5B).

### Functionalization of Microbubbles and Demonstration of Molecular Targeting

To demonstrate that monodisperse contrast agents could be used for molecular imaging, we functionalized our monodisperse contrast agents by incorporating biotinylated lipid into the microbubble shell. Many current molecular imaging methods involve conjugating biotinylated targeting ligands to contrast agents functionalized with biotin through an avidin linker.[1,7,34] After incubation with fluorescent avidin followed by washing, fluorescence microscopy confirmed the binding of avidin to the biotin-targeted microbubbles (Figure 5C). Adhesion of fluorescent avidin was not observed with non-biotinylated lipid microbubbles.

Alternatively, monodisperse microbubbles targeted to $\alpha_v\beta_3$ were created using lipids preconjugated to a cyclic RGD peptide. Optical microscopy demonstrated that RGD-targeted microbubbles remained adherent to an A375m monolayer. Targeted microbubbles were observed to maintain their monodisperse population characteristics after incubation with the cell monolayer and after rinses with PBS buffer (Figure 6).

### Acoustic Studies

Fifty-five echoes from monodisperse microbubbles and 109 echoes from polydisperse microbubbles were captured and compared. The standard deviation of the RMS echo amplitude for the polydisperse contrast agent was substantially greater than that for the monodisperse agent (Figure 7A). Additionally, the correlation of the echoes from the monodisperse microbubble population was significantly greater than that from the polydisperse microbubble population (0.86 vs 0.73; $p < .0001$) (Figure 7B).

## Discussion

Using microfluidics technology, stable DSPC–DSPE–PEG2000-coated and gas-filled contrast agents can be produced within the size range of commercial ultrasound contrast agents. The monolayer shell of monodisperse microbubbles produced consisted of a saturated acyl chain phospholipid and an emulsifier containing a hydrophilic polymer moiety and a lipid anchor. Fluorescence images showed phase coexistence of dark condensed-phase lipid domains surrounded by a bright expanded emulsifier-rich phase. These observations indicate coexistence of both lipid and an emulsifier in the microbubble shell, which enhances microbubble stability.[26]

We have demonstrated that these contrast agents can be functionalized to present biotin ligands in the shell to which antibodies or other targeting ligands can be secured through an avidin linker. Although the avidin-biotin chemistry presented here is a common approach for coupling targeting ligands to microbubbles for preclinical studies,[1,7,34] avidin is an immunogenic foreign protein and will need to be replaced by direct covalent coupling of the targeting ligand to the microbubble shell for clinical applications or longitudinal preclinical studies.[7]

By using lipids already incorporating an RGD-bioconjugate, targeted microbubbles can be made without additional avidin-biotin chemistry. We demonstrate the manufacture of RGD-targeted monodisperse microbubbles and subsequent adhesion of these microbubbles to $-_{v}\beta_{3}$-expressing cells. We have previously presented a more detailed analysis of the specificity of this targeting ligand.[11]

Through simulations, we have estimated that current imaging systems are optimized to interrogate only a small percentage of a polydisperse contrast agent population. In a normal (nontargeted) contrast-enhanced clinical ultrasound examination, this shortcoming may be of less importance because of the vast quantity of contrast agent microbubbles that are injected into the bloodstream (10 μL/kg—more than $1 \times 10^8$ microbubbles per examination).[20] Even so, only a fraction of this dose may ultimately reach the interrogated tissue to clearance in the lung and variations in local perfusion. However, in molecular imaging applications, the number of targeted contrast agents adherent at a target site is even further limited. The number of targeted contrast agents present in the target tissue after an accumulation period is dependent on the expression of target molecules and the likelihood of contrast agent binding and retention. These factors result in only a fraction of the injected dose retained in the vasculature at a target site. Previous researchers have observed low densities of retained agents in vivo, on the order of 5 to 25 per $mm^2$.[4,12,14] Hence, for applications in molecular imaging, it is important that the imaging system has maximum sensitivity to the targeted imaging agent.

The sensitivity of contrast ultrasound imaging may benefit from narrowing the diameter range of the contrast agent population in several ways. First, since the mean size of these agents can be easily changed, it is possible to have a contrast agent tailored specifically to the imaging frequency and application. We estimate from our simulations that, ideally, a several-fold increase in ultrasound sensitivity to contrast agents could be achieved by narrowing the size distribution alone (see Table 1). The use of a monodisperse contrast agent will also permit improvements in the signal processing strategies used for imaging. For example, most technologies, such as phase inversion, cadence contrast pulse sequencing, and sub-harmonic imaging, rely on the unique nonlinear acoustic response of microbubbles in response to an acoustic pulse to separate contrast echoes from tissue echoes. Given that microbubble response is directly related to diameter,[8,35] a uniform distribution of microbubbles will permit more precise tuning to the contrast agent signal (eg, tighter filter cutoffs, improved matched-filters), resulting in higher contrast to tissue ratios and better imaging sensitivity.

Initial acoustic studies demonstrated smaller standard deviation in RMS echo amplitude for monodisperse microbubble echoes compared with polydisperse microbubbles. These data confirm that the pulse shapes of the echoes from individual microbubbles in a monodisperse population are similar to each other. The radial oscillation and resulting acoustic response of a microbubble are directly related to its size.[8,35] Therefore, a smaller variation in terms of the amplitude, frequency, and pulse shape of microbubble echoes from monodisperse microbubbles is expected compared with echoes from polydisperse microbubbles. Experimental data indicate that the pulse to pulse echo correlation from monodisperse microbubbles is significantly higher than from polydisperse microbubbles.

In this study, we did not explore tuning the imaging frequency bandwidth to match the resonant frequency of the monodisperse contrast agents; hence, the mean echo amplitudes for monodisperse and polydisperse contrast agents were similar. Tuning the contrast agent resonant frequency to the imaging frequency will be explored in future studies.

Another possible advantage of the size-tuning contrast agents is the ability to alter biodistribution. Depending on the diameter of the contrast agent, preferred localization in vivo can be optimized or altered (J.R. Lindner, personal communication, 2007).

The gas core of current FDA-approved contrast agents is a mixture of air and a perfluorocarbon gas to reduce gas diffusion and provide enhanced stability over air alone. Future microbubble designs will involve the balance of air to perfluorocarbon concentration in which the partial pressure of perfluorocarbon will be adjusted to increase long-term stability.

### Limitations of Technology

The application of monodisperse contrast agents for molecular imaging opposed to polydisperse contrast will present increased sensitivity in applications in which the imaging bandwidth is tuned to the contrast agent frequency or contrast agent detection is based on echo correlation or matched filtering techniques. However, because of this tuning, one drawback would be that different contrast agents would be needed for different frequency ultrasound examinations.

One variable that is yet unknown is how the distribution of the monodisperse contrast agents will change in vitro. It is well known that contrast agents are sensitive to hydrostatic pressure and dissolved gas concentration, conditions that can vary in the circulation. Further experiments, perhaps through intravital microscopy, will be required to assess the change in the microbubble population in vivo.

Currently, the main limitation of this contrast agent production technique is that the microfluidics technology our group is using to produce monodisperse contrast agents has a low production rate. The commercial lipid-shelled contrast agent Definity consists of a lipid solution that produces over $1 \times 10^9$ contrast agents within 45 seconds of mechanical agitation. In contrast, our micro-fluidic chip technology can produce only on the order of $1 \times 10^6$ contrast agents/minute, still several orders of magnitude slower than current methods. However, one of the benefits of microfabricated systems such as ours is that they can be easily multiplexed. Future work will involve improving our technology to amplify the production rate.

## Conclusion

We propose the application of monodisperse contrast agents for molecular imaging applications owing to the ability to improve imaging sensitivity to the contrast agent population. Our experimental method illustrates the design of monodisperse lipid-coated microbubble contrast agents, which can be functionalized for molecular imaging. Control over microbubble size and production rate can be precisely tailored by changing gas pressure, liquid flow rate, and bulk liquid viscosity in our experimental system. Initial acoustic testing demonstrates higher correlation between echoes of nearly monodisperse microbubbles compared with that of polydisperse microbubbles, indicating that optimizing contrast agent distribution has the potential to enhance the sensitivity of contrast imaging. We anticipate even greater improvements in echo correlation with further optimization of the monodispersity of the microbubble population and tuning of the imaging system to echo the characteristics of monodisperse contrast agents.

## Acknowledgments

We are grateful to Prof. Katherine Ferrara and Prof. Alex Revzin for the use of their equipment and facilities. We also would like to thank Dr. Mark Borden for his thoughtful discussions and helpful insight regarding microbubble

development and Dr. Jonathan Lindner for conversations on the benefits of monodisperse contrast agents for molecular imaging.

Funding for this work was provided by the National Institutes of Health through the NIH Roadmap for Medical Research (Grant R21 EB005325) and the Center for Polymeric Interfaces and Macromolecular Assemblies (Grant NSF DMR 0213618).

## References

1. Lanza GM, Wallace KD, Scott MJ, et al. A novel site-targeted ultrasonic contrast agent with broad biomedical application. Circulation. 1996; 94:3334–40. [PubMed: 8989148]
2. Soman NR, Marsh JN, Hughes MS, et al. Acoustic activation of targeted liquid perfluorocarbon nanoparticles does not compromise endothelial integrity. IEEE Trans Nanobioscience. 2006; 5:69–75. [PubMed: 16805101]
3. Tiukinhoy-Laing SD, Buchanan K, Parikh D, et al. Fibrin targeting of tissue plasminogen activator-loaded echogenic liposomes. J Drug Target. 2007; 15:109–14. [PubMed: 17365281]
4. Leong-Poi H, Christiansen J, Klibanov AL, et al. Noninvasive assessment of angiogenesis by ultrasound and microbubbles targeted to alpha(v)-integrins. Circulation. 2003; 107:455–60. [PubMed: 12551871]
5. Rychak JJ, Lindner JR, Ley K, Klibanov AL. Deformable gas-filled microbubbles targeted to P-selectin. J Control Release. 2006; 114:288–99. [PubMed: 16887229]
6. Weller GE, Wong MK, Modzelewski RA, et al. Ultrasonic imaging of tumor angiogenesis using contrast microbubbles targeted via the tumor-binding peptide arginine-arginine-leucine. Cancer Res. 2005; 65:533–9. [PubMed: 15695396]
7. Klibanov AL, Rychak JJ, Yang WC, et al. Targeted ultrasound contrast agent for molecular imaging of inflammation in high-shear flow. Contrast Media Mol Imaging. 2006; 1:259–66. [PubMed: 17191766]
8. Dayton PA, Allen JS, Ferrara KW. The magnitude of radiation force on ultrasound contrast agents. J Acoust Soc Am. 2002; 112:2183–92. [PubMed: 12430830]
9. Behm CZ, Lindner JR. Cellular and molecular imaging with targeted contrast ultrasound. Ultrasound Q. 2006; 22:67–72. [PubMed: 16641795]
10. Lanza GM, Wickline SA. Targeted ultrasonic contrast agents for molecular imaging and therapy. Curr Probl Cardiol. 2003; 28:625–53. [PubMed: 14691443]
11. Dayton PA, Pearson D, Clark J, et al. Ultrasonic analysis of peptide- and antibody-targeted microbubble contrast agents for molecular imaging of {alpha}v{beta}3-expressing cells. Mol Imaging. 2004; 3:125. [PubMed: 15296677]
12. Schumann PA, Christiansen JP, Quigley RM, et al. Targeted-microbubble binding selectively to GPIIb IIIa receptors of platelet thrombi. Invest Radiol. 2002; 37:587–93. [PubMed: 12393970]
13. Lindner JR, Dayton PA, Coggins MP, et al. Non-invasive assessment of inflammation using ultrasound detection of phagocytosed microbubbles. Circulation. 2000; 102:531–8. [PubMed: 10920065]
14. Ellegala DB, Leong-Poi H, Carpenter JE, et al. Imaging tumor angiogenesis with contrast ultrasound and microbubbles targeted to alpha(v)beta3. Circulation. 2003; 108:336–41. [PubMed: 12835208]
15. Weller G, Wong M, Modzelewski RA, et al. Ultrasonic imaging of tumor angiogenesis using contrast microbubbles targeted via the tumor-binding peptide arginine-arginine-leucine. Cancer Res. 2005; 65:533–9. [PubMed: 15695396]
16. Zhao S, Borden M, Bloch SH, et al. Radiation-force assisted targeting facilitates ultrasonic molecular imaging. Mol Imaging. 2004; 3:135–48. [PubMed: 15530249]
17. Rychak JJ, Klibanov AL, Ley KF, Hossack JA. Enhanced targeting of ultrasound contrast agents using acoustic radiation force. Ultrasound Med Biol. 2007; 33:1132–9. [PubMed: 17445966]
18. Zhao S, Kruse DE, Ferrara KW, Dayton PA. Acoustic response from adherent targeted contrast agents. J Acoust Soc Am. 2006; 120:EL63–9. [PubMed: 17225437]
19. Zhao S, Kruse D, Ferrara K, Dayton PA. Selective imaging of adherent targeted ultrasound contrast agents. Phys Med Biol. 2007; 52:2055–72. [PubMed: 17404455]

20. Hughes MS, Klibanov AL, Marsh JN, et al. Broadband time-domain reflectometry measurement of attenuation and phase velocity in highly attenuating suspensions with application to the ultrasound contrast medium Albunex. J Acoust Soc Am. 2000; 108:813–20. [PubMed: 10955648]
21. Ganan-Calvo AM, Gordillo JM. Perfectly monodisperse microbubbling by capillary flow focusing. Phys Rev Lett. 2001; 87:274501–4. [PubMed: 11800883]
22. Garstecki P, Ganan-Calvo AM, Whitesides GM. Formation of bubbles and droplets in microfluidic systems. Bull Pol Acad Sci Tech Sci. 2005; 53:361–72.
23. Morgan KE, Allen JS, Dayton PA, et al. Experimental and theoretical evaluation of microbubble behavior: effect of transmitted phase and bubble size. IEEE Trans Ultrason Ferroelectr Freq Control. 2000; 47:1494–509. [PubMed: 18238696]
24. Hettiarachchi K, Talu E, Longo ML, et al. On-chip generation of microbubbles as a practical technology for manufacturing contrast agents for ultrasonic imaging. Lab Chip. 2007; 7:463–8. [PubMed: 17389962]
25. Talu E, Hettiarachchi K, Nguyen H, et al. Lipid-stabilized monodisperse microbubbles produced by flow focusing for use as ultrasound contrast agents. 2006:1568–1571.10.1109/ULTSYM.2006.398
26. Borden MA, Pu G, Runner GJ, Longo ML. Surface phase behavior and microstructure of lipid/PEG-emulsifier monolayer-coated microbubbles. Colloids Surf B. 2004; 35:209–23.
27. Klibanov AL, Rasche PT, Hughes MS, et al. Detection of individual microbubbles of ultrasound contrast agents: imaging of free-floating and targeted bubbles. Invest Radiol. 2004; 39:187–95. [PubMed: 15076011]
28. Weller G, Villanueva FS, Tom EM, Wagner WR. Targeted ultrasound contrast agents: in vitro assessment of endothelial dysfunction and multi-targeting to ICAM-1 and sialyl Lewisx. Biotechnol Bioeng. 2005; 92:780–8. [PubMed: 16121392]
29. Unger EC, McCreery TP, Sweitzer RH, et al. Acoustically active lipospheres containing paclitaxel: a new therapeutic ultrasound contrast agent. Invest Radiol. 1998; 33:886–92. [PubMed: 9851823]
30. Bloch SH, Dayton PA, Ferrara KW. Targeted imaging using ultrasound contrast agents. Progess and opportunities for clinical and research applications. IEEE Eng Med Biol Mag. 2004; 23:18–29. [PubMed: 15565796]
31. Talu E, Lozano MM, Powell RL, et al. Long-term stability by lipid coating monodisperse microbubbles formed by a flow-focusing device. Langmuir. 2006; 22:9487–90. [PubMed: 17073468]
32. Klibanov AL, Hughes MS, Villanueva FS, et al. Targeting and ultrasound imaging of microbubble-based contrast agents. Magma. 1999; 8:177–84. [PubMed: 10504045]
33. Borden MA, Martinez GV, Ricker J, et al. Lateral phase separation in lipid-coated microbubbles. Langmuir. 2006; 22:4291–7. [PubMed: 16618177]
34. Villanueva FS, Lu E, Bowry S, et al. Myocardial ischemic memory imaging with molecular echocardiography. Circulation. 2007; 115:345–52. [PubMed: 17210843]
35. Chomas JE, Dayton P, May D, Ferrara K. Threshold of fragmentation for ultrasonic contrast agents. J Biomed Opt. 2001; 6:141–50. [PubMed: 11375723]

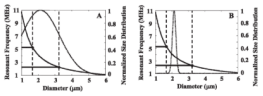

**Figure 1.**
Overlap between resonant frequencies in a microbubble population and the −6 dB bandwidth of a 3.8 MHz 80% bandwidth transducer. *A*, Microbubble population similar to commercially available lipid-encapsulated contrast agents (2.1 ± 1.1 μm). *B*, "Nearly monodisperse" microbubble population in which the mean diameter has a resonant frequency that matches the transducer center frequency, with a standard deviation of 5% of the mean diameter.

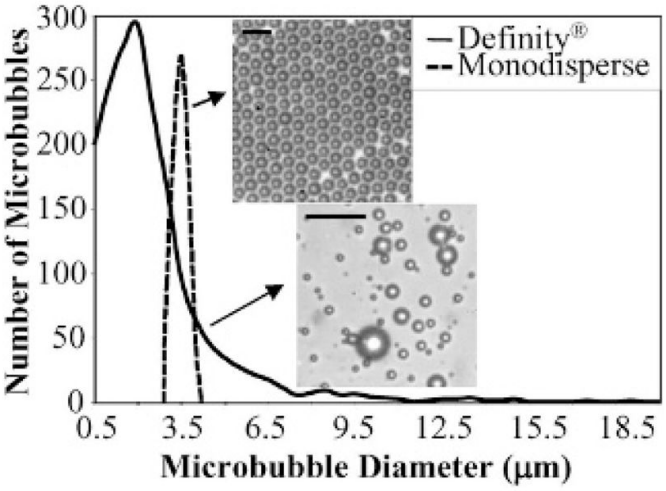


**Figure 2.**

Size distribution of contrast agents manufactured in our laboratory (3.7 μm with a standard deviation of 0.2 μm in this case) in contrast to the commercially available contrast agent Definity (2.7 μm with a standard deviation of 2.0 μm). The scale bar represents 10 μm.

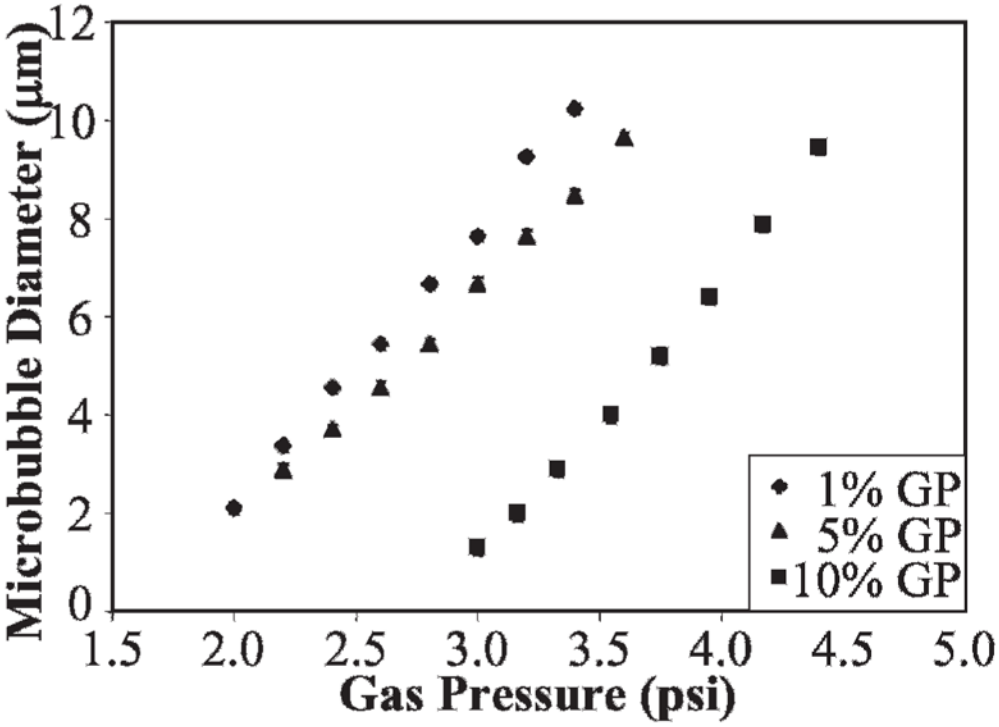


**Figure 3.**
Size dependence of microbubbles on gas pressure and the bulk liquid viscosity (increased with glycerine and propylene glycol [GP]) by keeping the liquid flow rate constant (30 μL/min).

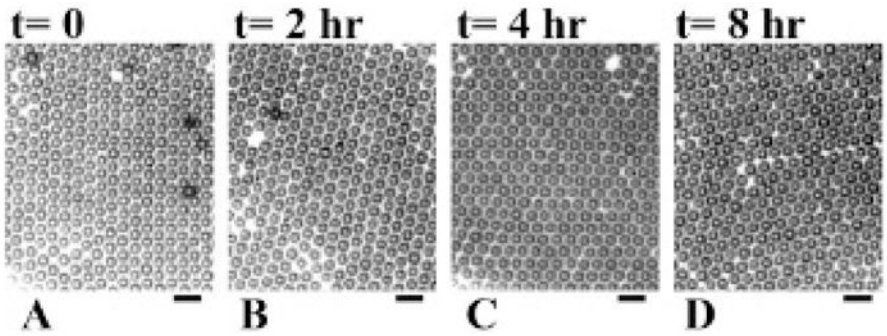


**Figure 4.**

Microscope images of microbubbles recorded at different times illustrating stability: *A*, t = 0; *B*, t = 2 hours; *C*, t = 4 hours; *D*, t = 8 hours. The microbubbles have a mean diameter of 3.7 μm with a standard deviation of 0.2 μm. The scale bar represents 10 μm.

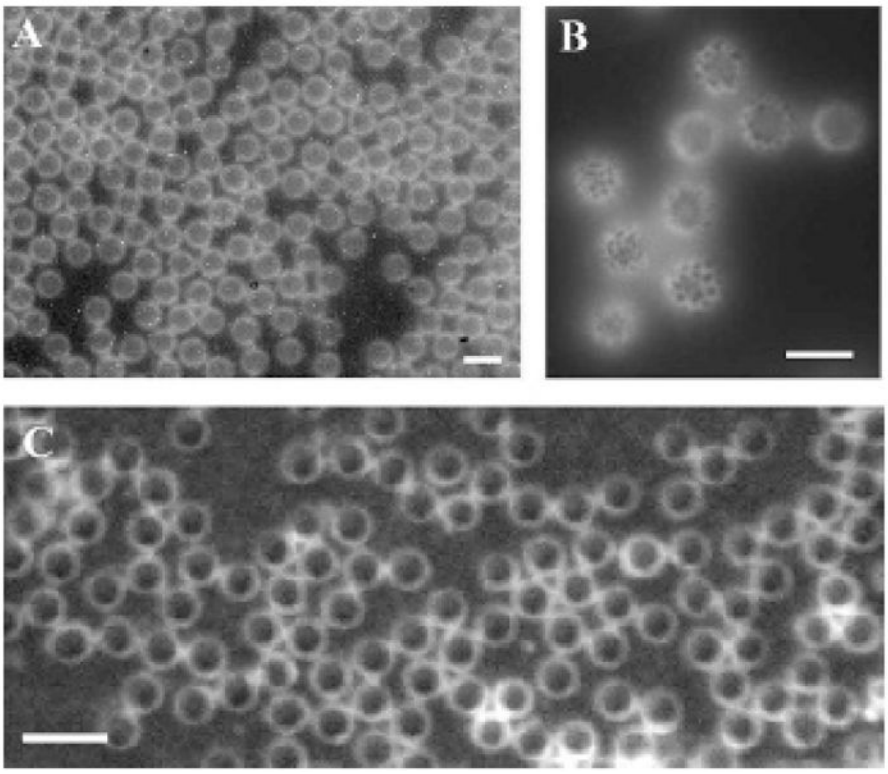


**Figure 5.**
*A* and *B*, Images of a population of lipid-coated monodisperse microbubbles incorporating DiI, illustrating the lipid and emulsifier phase coexistence. The scale bar represents 10 μm. C, Biotin-functionalized monodisperse microbubbles made without DiI, incorporating fluorescent avidin. Scale bar represents 5 μm.

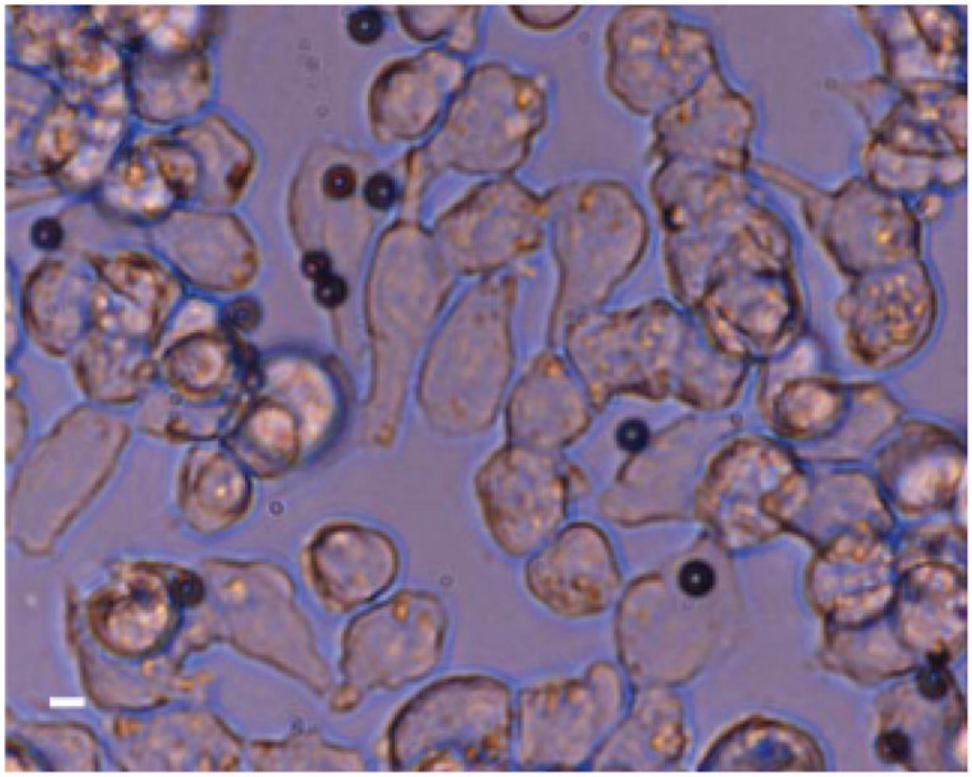

**Figure 6.**
Monodisperse RGD-targeted microbubbles adherent to an $\alpha_v\beta_3$-expressing A375m cell monolayer. Scale bar represents 5 μm.

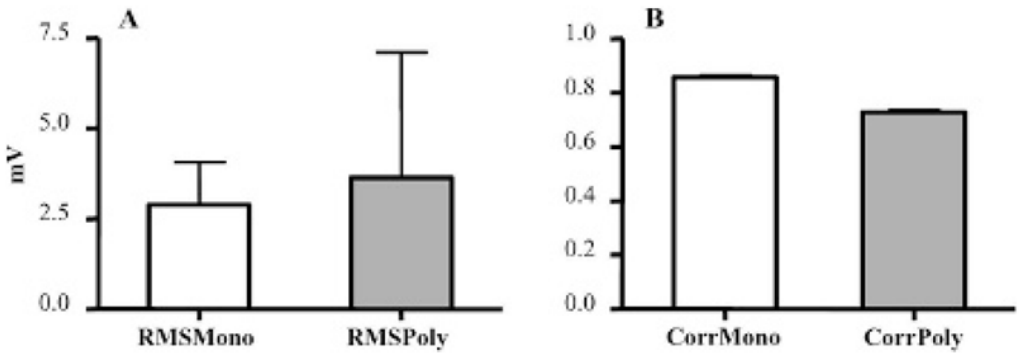


**Figure 7.**

*A*, The amplitude of scattered echoes from individual mono-disperse microbubbles had less standard deviation than polydisperse microbubble echoes. *B*, Echoes of individual microbubbles were more correlated for monodisperse micro-bubbles compared with polydisperse microbubbles. RMS = root mean square.

**Table 1**

Percent of Microbubbles with Resonant Frequencies within −6 dB of 80% Bandwidth Imaging Transducer

| Center Frequency (MHz) | Polydisperse (%) | Monodisperse (%) |
|---|---|---|
| 1 | 8 | 100 |
| 2 | 29 | 100 |
| 3 | 45 | 100 |
| 4 | 44 | 100 |
| 5 | 36 | 100 |
| 6 | 32 | 100 |
| 7 | 23 | 100 |
| 8 | 22 | 100 |
| 9 | 23 | 100 |
| 10 | 18 | 100 |

**Table 2**

Production Rate Dependence on Gas Pressure and Glycerin–Propylene Glycol Vol % at a Constant Liquid Flow Rate of 50 μL/min

| Gas Pressure (psi) | Glycerin and Propylene Glycol (vol %) | Production Rate(bubbles/s) |
|---|---|---|
| 3 | 1 | 500 ± 10 |
| 5 | 1 | 50,000 ± 100 |
| 3 | 5 | 300 ± 5 |
| 3 | 10 | 100 ± 3 |
| 5 | 10 | 40,000 ± 100 |